LETTER

doi:10.1038/nature09567

Bose–Einstein condensation of photons in an optical microcavity

Jan Klaers, Julian Schmitt, Frank Vewinger & Martin Weitz

Bose–Einstein condensation (BEC)—the macroscopic ground-state accumulation of particles with integer spin (bosons) at low temperature and high density—has been observed in several physical systems[1–9], including cold atomic gases and solid-state quasiparticles. However, the most omnipresent Bose gas, blackbody radiation (radiation in thermal equilibrium with the cavity walls) does not show this phase transition. In such systems photons have a vanishing chemical potential, meaning that their number is not conserved when the temperature of the photon gas is varied[10]; at low temperatures, photons disappear in the cavity walls instead of occupying the cavity ground state. Theoretical works have considered thermalization processes that conserve photon number (a prerequisite for BEC), involving Compton scattering with a gas of thermal electrons[11] or photon–photon scattering in a nonlinear resonator configuration[12,13]. Number-conserving thermalization was experimentally observed[14] for a two-dimensional photon gas in a dye-filled optical microcavity, which acts as a 'white-wall' box. Here we report the observation of a Bose–Einstein condensate of photons in this system. The cavity mirrors provide both a confining potential and a non-vanishing effective photon mass, making the system formally equivalent to a two-dimensional gas of trapped, massive bosons. The photons thermalize to the temperature of the dye solution (room temperature) by multiple scattering with the dye molecules. Upon increasing the photon density, we observe the following BEC signatures: the photon energies have a Bose–Einstein distribution with a massively populated ground-state mode on top of a broad thermal wing; the phase transition occurs at the expected photon density and exhibits the predicted dependence on cavity geometry; and the ground-state mode emerges even for a spatially displaced pump spot. The prospects of the observed effects include studies of extremely weakly interacting low-dimensional Bose gases[9] and new coherent ultraviolet sources[15].

Fifty years ago, the invention of the laser provided us with a source of coherent light. In a laser, optical gain is achieved under conditions where both the state of the gain medium and the state of the light field are far removed from thermal equilibrium[16]. The realization of a light source with a macroscopically populated photon mode that is not the consequence of a laser-like gain, but is rather due to an equilibrium phase transition of photons has so far been prevented by the lack of a suitable number-conserving thermalization process[17]. For strongly coupled mixed states of photons and excitons (exciton polaritons), a thermalization process induced by interparticle interactions between excitons has been reported to lead to a (quasi-)equilibrium BEC of polaritons[5–7]. In the present work, rapid decoherence due to frequent collisions of dye molecules with the solvent prevents coherent energy exchange between photons and dye molecules and therefore the condition of strong matter–field coupling is not met[18,19]. We can therefore assume the relevant particles to be well described as photons instead of polaritons.

Our experiment confines photons in a curved-mirror optical microresonator filled with a dye solution, in which photons are repeatedly absorbed and re-emitted by the dye molecules. The small distance of 3.5 optical wavelengths between the mirrors causes a large frequency spacing between adjacent longitudinal modes (the free spectral range is 7×10^{13} Hz), comparable with the spectral width of the dye (see Fig. 1a), and modifies spontaneous emission such that the emission of photons with a given longitudinal mode number, $q = 7$ in our case, dominates over other emission processes. In this way, the longitudinal mode number is frozen out and the remaining transverse modal degrees of freedom make the photon gas effectively two-dimensional. Moreover, the dispersion relation becomes quadratic (that is, non-relativistic), as indicated in Fig. 1b, with the frequency of the $q = 7$ transverse ground mode (TEM_{00}) acting as a low-frequency cut-off with $\omega_{\text{cut-off}} \cong 2\pi \times 5.1 \times 10^{14}$ Hz. The curvature of the mirrors

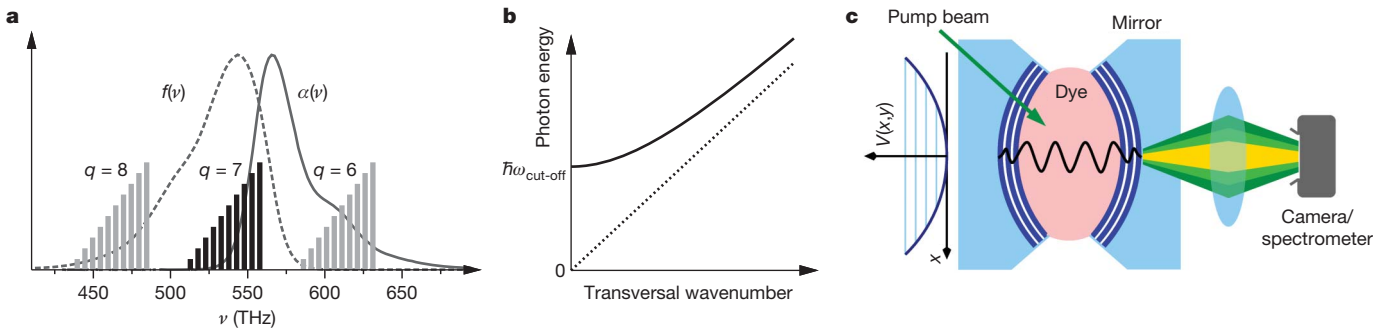

Figure 1 | Cavity mode spectrum and set-up. a, Schematic spectrum of cavity modes and (relative) absorption coefficient $\alpha(\nu)$ and fluorescence strength $f(\nu)$ of rhodamine 6G dye versus frequency ν. Transverse modes belonging to the manifold of longitudinal mode number $q = 7$ are shown by black lines, and those of other longitudinal mode numbers in grey. The degeneracy of a given transversal energy is indicated by the height of the bars. **b**, Dispersion relation of photons in the cavity (solid line), with fixed longitudinal mode number ($q = 7$), and the free photon dispersion (dashed line). **c**, Scheme of the experimental set-up. The trapping potential $V(x,y)$ for the two-dimensional photon gas imposed by the curved mirrors—see the third term in equation (2) of the Methods—is indicated on the left hand side.

Institut für Angewandte Physik, Universität Bonn, Wegelerstrasse 8, 53115 Bonn, Germany.

induces a harmonic trapping potential for the photons (see Methods). This is indicated in Fig. 1c, along with a scheme of the experimental set-up.

Thermal equilibrium of the photon gas is achieved by absorption and re-emission processes in the dye solution, which acts as heat bath and equilibrates the transverse modal degrees of freedom of the photon gas to the (rovibrational) temperature of the dye molecules (see Methods). The photon frequencies will accumulate within a range $k_B T/\hbar$ ($\cong 2\pi \times 6.3 \times 10^{12}$ Hz at room temperature, where $\hbar$ is the reduced Planck constant) above the low-frequency cut-off. In contrast to the case of a blackbody radiator, for which the photon number is determined by temperature (Stefan–Boltzmann law), the number of (optical) photons in our microresonator is not altered by the temperature of the dye solution, because purely thermal excitation is suppressed by a factor of the order of $\exp(\hbar\omega_{\text{cut-off}}/k_B T) \approx \exp(-80)$. The thermalization process thus conserves the average photon number.

Our system is formally equivalent to an ideal gas of massive bosons having an effective mass $m_{\text{ph}} = \hbar\omega_{\text{cut-off}}/c^2 \cong 6.7 \times 10^{-36}$ kg (where subscript 'ph' stands for 'photon') that are moving in the transverse resonator plane, harmonically confined with a trapping frequency $\Omega = c/\sqrt{D_0 R/2} \cong 2\pi \times 4.1 \times 10^{10}$ Hz (see Methods), with c as the speed of light in the medium, $D_0 \cong 1.46$ μm the mirror separation and $R \cong 1$ m the radius of curvature. A harmonically trapped two-dimensional ideal gas exhibits BEC at finite temperature[20,21], in contrast to the two-dimensional homogeneous case. We therefore expect a BEC when the photon wave packets spatially overlap at low temperatures or high densities, that is, the phase space density $n\lambda_{\text{th}}^2$ (where subscript 'th' stands for 'thermal') exceeds a value near unity. Here n denotes the number density in photons per area, and $\lambda_{\text{th}} = h/\sqrt{2\pi m_{\text{ph}} k_B T} \cong 1.58$ μm (defined in analogy to, for example, a gas of atoms[17]) is the de Broglie wavelength associated with the thermal motion in the resonator plane. We note that $\lambda_{\text{th}} = 2\sqrt{\pi}/k_{r,\text{ r.m.s.}}$, where $k_{r,\text{ r.m.s.}} = \sqrt{\langle k_r^2 \rangle_T}$ is the root mean square (r.m.s.) transverse component of the photon wavevector at temperature T. The precise onset of BEC in this two-dimensional, harmonically trapped system can be determined from a statistical description using a Bose–Einstein distributed occupation of trap levels[14,20,21], giving a critical particle number of:

$$N_c = \frac{\pi^2}{3}\left(\frac{k_B T}{\hbar\Omega}\right)^2 \qquad (1)$$

At room temperature ($T = 300$ K), we arrive at $N_c \cong 77{,}000$. It is interesting to note that both the thermal energy $k_B T$ and the trap level spacing $\hbar\Omega$ are roughly a factor of 10^9 above the corresponding values in atomic physics BEC experiments[2–4], but that the ratio $k_B T/\hbar\Omega \cong 150$, corresponding to the mean excitation value per axis, is quite comparable.

By pumping the dye with an external laser we add to a reservoir of electronic excitations that exchanges particles with the photon gas, in the sense of a grand-canonical ensemble. The pumping is maintained throughout the measurement to compensate for losses due to coupling into unconfined optical modes, finite quantum efficiency and mirror losses. In a steady state, the average photon number will be $N_{\text{ph}} = N_{\text{exc}}\tau_{\text{ph}}/\tau_{\text{exc}}$, where N_{exc} is the number of molecular excitations, τ_{exc} is their electronic lifetime in the resonator (of the order of a nanosecond) and $\tau_{\text{ph}} \cong 20$ ps is the average time between emission and reabsorption of a photon. For a detailed description of the thermalization, it is important to realize that it originates from particle exchange with a reservoir that is in equilibrium. The reservoir is characterized by rovibrational molecular states that are highly equilibrated both in the lower and in the upper electronic levels owing to subpicosecond relaxation[22] induced by frequent collisions with solvent molecules. This process efficiently decorrelates the states of absorbed and emitted photons, and leads to a temperature-dependent absorption and emission spectral profile that is responsible for the thermalization. To relax both spatially and spectrally to an equilibrium distribution, a photon has to scatter several times off molecules before being lost. In previous work, we have shown that the photon gas in the dye-filled microcavity system can be well described by a thermal equilibrium distribution, showing that photon loss is sufficiently slow[14]. To avoid excessive population of dye molecule triplet states and heat deposition, the pump beam is acousto-optically chopped to 0.5-μs pulses, which is at least two orders of magnitude above the described timescales, with 8-ms repetition time.

Typical room-temperature spectra for increasing pumping power are given in Fig. 2a (recorded using rhodamine 6G dye solved in methanol, 1.5×10^{-3} M). At low pumping and correspondingly low intracavity power we observe a spectrally broad emission, which is in good agreement with a room-temperature Boltzmann distribution of photon energies above the cavity cut-off[14]. With increasing pump power the maximum of the spectral distribution shifts towards the cavity cut-off, that is, it more resembles a Bose–Einstein distribution function. For a pumping power above threshold, a spectrally sharp peak at the frequency of the cavity cut-off is observed, while the thermal wing shows saturation. The described signatures are in good agreement with theoretical spectra based on Bose–Einstein distributed transversal excitations (inset of Fig. 2a). At the phase transition the power inside the resonator is $P_{c,\text{ exp}} = (1.55 \pm 0.60)$ W, corresponding to a critical photon number of $(6.3 \pm 2.4) \times 10^4$. This value still holds when rhodamine is replaced by perylene-diimide (PDI) solved in acetone (0.75 g l^{-1}); that is, for both dyes the measured critical number is in agreement with the value predicted for a BEC of photons (equation (1)).

Spatial images of the photon gas below and slightly above criticality are shown in Fig. 2b. In either case the lower energetic (yellow) photons are bound to the trap centre while the higher energetic (green) photons appear at the outer trap regions. Above the critical photon number a bright spot is visible in the trap centre with a full width at half-maximum (FWHM) diameter of (14 ± 3) μm, indicating a macroscopically populated TEM_{00}-mode (expected diameter 12.2 μm). Figure 2c shows normalized spatial intensity profiles along one axis for increasing pumping power near the critical value. Interestingly, we observe that the mode diameter enlarges with increasing condensate fraction, as shown in Fig. 2d. This effect is not expected for an ideal gas of photons. In principle, this could be due to a Kerr nonlinearity in the dye solution, but the most straightforward explanation is a weak repulsive optical self-interaction from thermal lensing in the dye (which can be modelled by a mean-field interaction; see Methods). From the increase of the mode diameter we can estimate the magnitude of this effective repulsive interaction, yielding a dimensionless interaction parameter of $\tilde{g} \approx (7 \pm 3) \times 10^{-4}$. This is much below the values $\tilde{g} = 10^{-2} \ldots 10^{-1}$ reported for two-dimensional atomic physics quantum gas experiments and also below the value at which Kosterlitz–Thouless physics, involving 'quasi-long-range' order, is expected to become relevant[23]. The latter is supported by an experiment directing the condensate peak through a shearing interferometer, in which we have not seen signatures of the phase blurring expected for a Kosterlitz–Thouless phase[24].

We have tested for a dependence of the BEC threshold on the resonator geometry. From equation (1) we expect a critical optical power $P_c = (\pi^2/12)(k_B T)^2(\omega_{\text{cut-off}}/\hbar c) R$, which grows linearly with the mirror radius of curvature R and is independent of the longitudinal mode number q. Figure 3a and the lower panel of Fig. 3b show corresponding measurements of the critical power, with results in good agreement with both the expected absolute values and the expected scaling. The upper panel of Fig. 3b gives the required optical pump power to achieve the phase transition versus the number of longitudinal modes, showing a decrease because of stronger pump power absorbance for larger mirror spacing. This is in strong contrast to results reported from 'thresholdless' optical microlasers, for which an increase of the threshold pumping power was observed[25,26]. For a macroscopic laser a fixed value of the pump intensity is required to reach inversion.

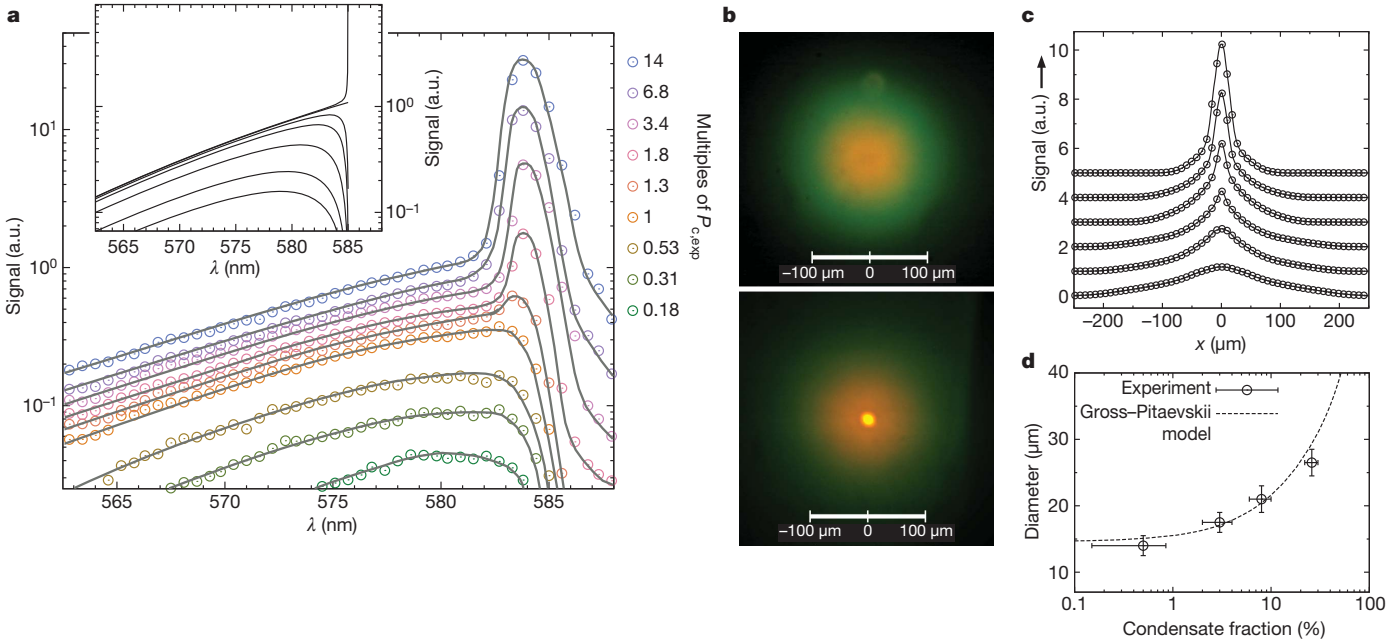

Figure 2 | Spectral and spatial intensity distribution. **a**, Spectral intensity distributions (connected circles) transmitted through one cavity mirror, as measured with a spectrometer, for different pump powers (see colour key). The intracavity power (in units of $P_{c,exp} = (1.55 \pm 0.60)$ W) is derived from the power transmitted through one cavity mirror. A spectrally sharp condensate peak at the cavity cut-off is observed above a critical power level, with a width limited by the spectrometer resolution. The inset gives theoretical spectra (solid lines) based on a Bose–Einstein distribution of photons for different particle numbers at room temperature[14]. a.u., arbitrary units. **b**, Images of the spatial radiation distribution transmitted through one cavity mirror both below (upper panel) and above (lower panel) criticality, showing a macroscopically occupied TEM_{00}-mode for the latter case. **c**, **d**, Cut through the centre of the intensity distribution for increasing optical pump powers (**c**) and width of the condensate peak versus condensate fraction, along with a theoretical model based on the Gross–Pitaevskii equation with an interaction parameter $\tilde{g} = 7 \times 10^{-4}$ (Methods) (**d**). Error bars are the systematic calibration uncertainties. $q = 11$ for **c** and **d**. All other measurements use $q = 7$.

Finally, we have investigated the condensation for a spatially mismatched pumping spot. Owing to the thermal redistribution of photons we expect that even a spatially displaced pump beam can provide a sufficiently high photon density at the trap centre to reach the phase transition. This effect is not known in lasers, but is observed in the framework of polariton condensation[7]. For our measurement, the pump beam (diameter about 35 μm) was displaced at about 50 μm from the trap centre. Figure 4 shows a series of spatial intensity profiles recorded for a fixed pumping power and for different values of the cavity cut-off wavelength $\lambda_{cut\text{-}off}$, which tunes the degree of thermalization[14]. The lower graph gives results recorded with $\lambda_{cut\text{-}off} \cong 610$ nm, for which the maximum fluorescence is centred at the position of the pump spot (shown by a dashed line). The weak reabsorption in this wavelength range prevents efficient photon thermalization. When the cut-off is moved to shorter wavelengths, the stronger reabsorption in this wavelength range leads to increasingly symmetric photon distributions

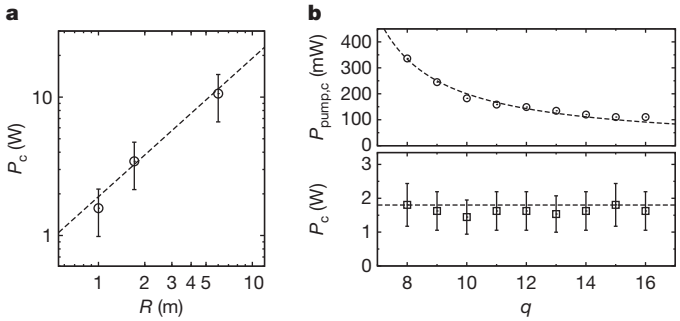

Figure 3 | Critical power. **a**, Intracavity power at criticality for different curvatures of the cavity mirrors. The dashed line shows the theoretical expectation based on equation (1). **b**, Intracavity power at criticality (lower panel) versus longitudinal mode number q. The upper panel shows the required optical pump power $P_{pump,c}$ (circles) along with a fit $P_{pump,c} \propto (q - q_0)^{-1}$ yielding $q_0 = 4.77 \pm 0.25$. For this we assume an inverse proportionality to the absorption length in the dye $q - q_0$, where q_0 incorporates an effective penetration depth into the cavity mirrors. The above value for q_0 is in good agreement with an independent measurement of the pump power transmission, yielding $q_0 = 4.77 \pm 0.17$. Error bars are systematic uncertainties.

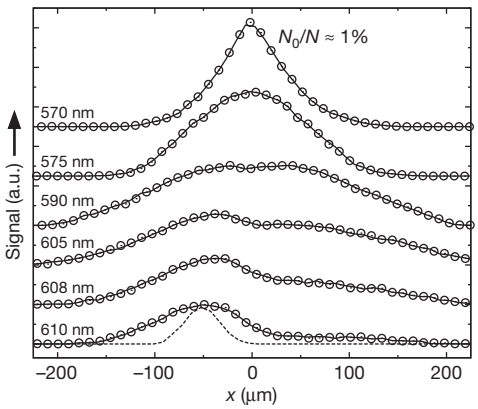

Figure 4 | Spatial redistribution of photons. Intensity profiles recorded with a pump beam spot (diameter about 35 μm) spatially displaced by 50 μm from the trap centre, for different cut-off wavelengths. For a cut-off wavelength of 610 nm (bottom profile), where reabsorption is weak, the emitted radiation is centred at the position of the pump spot, whose profile is shown by the dashed line (measured by removing one of the cavity mirrors). When tuning the cavity cut-off to shorter wavelength values, where the reabsorption efficiency is increased, light is redistributed towards the trap centre. For data recorded with a 570 nm cut-off wavelength (top profile), a cusp appears, corresponding to a partly condensed state with a condensate fraction N_0/N of about 1%.

around the trap centre. For a cavity cut-off near 570 nm we observe a small bright spot at the position of the TEM_{00}-mode. The corresponding cusp in the intensity profile of Fig. 4 indicates a condensate fraction of roughly $N_0/N \approx 1\%$. These measurements show that owing to the photon thermalization, BEC can be achieved even when the pumping intensity at the position of the ground state mode is essentially zero.

To conclude, evidence for a BEC of photons was obtained from (1) the spectral distribution that shows Bose–Einstein distributed photon energies, including a macroscopically occupied ground state, (2) the observed onset of the phase transition, which occurs both at the predicted absolute value of the photon number and shows the expected scaling with resonator geometry, and (3) the condensation appearing at the trap centre even for a spatially disjunct pump spot. It is instructive to discuss the relation of a photon BEC to microlasers, which also use high finesse cavities to capture the emission of excited-state atoms and molecules in a small volume[25–27]. The low lasing thresholds and potentially inversionless oscillation of microlasers, however, result from a high coupling efficiency of spontaneous photons into a single cavity mode—which is not the case here, as is evident from the observed highly multimodal emission below criticality. The main difference between a laser and BEC remains that the BEC (in contrast to the laser) is in thermal equilibrium, with the macroscopically populated mode being a consequence of equilibrium Bose statistics.

An interesting consequence of a grand-canonical particle exchange between photon gas and the reservoir of excited state dye molecules is that unusually large number fluctuations of the condensed phase could occur[28]. We expect that the concept of photon condensation holds promise for the exploration of novel states of light, and for light sources in new wavelength regimes.

METHODS SUMMARY

Preparation of photon gas. Photons are confined in an optical microresonator consisting of two curved dielectric mirrors with >99.997% reflectivity, filled with dye solution. The dye is pumped with a laser beam near 532 nm wavelength (about 70 μm diameter except for Fig. 4) directed at an angle of 45° to the optical axis, exploiting a reflectivity minimum of the mirrors. The trapped photon gas thermalizes to the rovibrational temperature T of the dye solution by repeated absorption and emission processes, as follows from a detailed balance condition[14] fulfilled in media obeying the Kennard–Stepanov relation[29] $f_T(\omega)/\alpha_T(\omega) \propto \omega^3 e^{-\hbar\omega/k_B T}$, which describes a temperature-dependent frequency scaling of absorption coefficient $\alpha_T(\omega)$ versus emission strength $f_T(\omega)$. We note that this equilibrium between photons and the dye solution is reminiscent of Einstein's description of the heat contact between radiation and a Doppler-broadened gas[30].

Photon dispersion in cavity and optical self-interaction. The photon energy in the resonator as a function of transversal (k_r) and longitudinal (k_z) wavenumber reads $E = \hbar c\sqrt{k_z^2 + k_r^2}$, where c denotes the speed of light in the medium. The boundary conditions yield $k_z(r) = q\pi/D(r)$, where $D(r) = D_0 - 2(R - \sqrt{R^2 - r^2})$ gives the mirror separation at distance r from the optical axis. For fixed longitudinal mode number q and in paraxial approximation ($r \ll R, k_r \ll k_z$), one arrives at the dispersion of a particle with nonvanishing mass $m_{ph} = \hbar k_z(0)/c = \hbar\omega_{cut\text{-}off}/c^2$, with its motion restricted to the (two-dimensional) transverse resonator plane under harmonic confinement with trapping frequency $\Omega = c\sqrt{2/D_0 R}$; see ref. 14. A possible self-interaction of photons (Kerr lensing or thermal lensing in the limit of neglibile transverse heat flow) can be incorporated by $n(r) = n_0 + n_2 I(r)$, where $I(r)$ is the optical intensity and n_0 ($\cong 1.33$ for methanol) and n_2 are the linear and nonlinear indices of refraction respectively, yielding:

$$E \cong m_{ph}c^2 + \frac{(\hbar k_r)^2}{2m_{ph}} + \frac{1}{2}m_{ph}\Omega^2 r^2 - m_{ph}c^2\frac{n_2}{n_0}I(r) \qquad (2)$$

The latter term resembles a mean-field interaction familiar from the Gross–Pitaevskii equation for atomic BECs, which, using a dimensionless interaction parameter[23] $\tilde{g} = -(m_{ph}^4 c^6 n_2)/(2\pi\hbar^3 n_0 q)$ and wavefunction $\psi(r)$ with $I(r) = (m_{ph}c^2)^2(hq)^{-1}N_0|\psi(r)|^2$, can be written in the more familiar form:

$$E_{int} = (\hbar^2/m_{ph})\tilde{g}N_0|\psi(r)|^2$$

Received 12 July; accepted 6 October 2010.

1. Einstein, A. Quantentheorie des einatomigen idealen Gases. Zweite Abhandlung. *Sitz. ber. Preuss. Akad. Wiss.* **1,** 3–14 (1925).
2. Anderson, M. H., Ensher, J. R., Matthews, M. R., Wieman, C. E. & Cornell, E. A. Observation of Bose–Einstein condensation in a dilute atomic vapor. *Science* **269,** 198–201 (1995).
3. Davis, K. B. *et al.* Bose-Einstein condensation in a gas of sodium atoms. *Phys. Rev. Lett.* **75,** 3969–3973 (1995).
4. Bradley, C. C., Sackett, C. A. & Hulet, R. G. Bose-Einstein condensation of lithium: observation of limited condensate number. *Phys. Rev. Lett.* **78,** 985–989 (1997).
5. Deng, H., Weihs, G., Santori, C., Bloch, J. & Yamamoto, Y. Condensation of semiconductor microcavity exciton polaritons. *Science* **298,** 199–202 (2002).
6. Kasprzak, J. *et al.* Bose–Einstein condensation of exciton polaritons. *Nature* **443,** 409–414 (2006).
7. Balili, R., Hartwell, V., Snoke, D., Pfeiffer, L. & West, K. Bose-Einstein condensation of microcavity polaritons in a trap. *Science* **316,** 1007–1010 (2007).
8. Demokritov, S. O. *et al.* Bose-Einstein condensation of quasi-equilibrium magnons at room temperature under pumping. *Nature* **443,** 430–433 (2006).
9. Griffin, A., Snoke, D. W. & Stringari, S. (eds) *Bose-Einstein Condensation* (Cambridge University Press, 1995).
10. Huang, K. *Statistical Mechanics* 2nd edn 293–294 (Wiley, 1987).
11. Zel'dovich, Y. B. & Levich, E. V. Bose condensation and shock waves in photon spectra. *Sov. Phys. JETP* **28,** 1287–1290 (1969).
12. Chiao, R. Y. Bogoliubov dispersion relation for a 'photon fluid': is this a superfluid? *Opt. Commun.* **179,** 157–166 (2000).
13. Bolda, E. L., Chiao, R. Y. & Zurek, W. H. Dissipative optical flow in a nonlinear Fabry-Pérot cavity. *Phys. Rev. Lett.* **86,** 416–419 (2001).
14. Klaers, J., Vewinger, F. & Weitz, M. Thermalization of a two-dimensional photonic gas in a 'white-wall' photon box. *Nature Phys.* **6,** 512–515 (2010).
15. Jonkers, J. High power extreme ultra-violet (EUV) light sources for future lithography. *Plasma Sources Sci. Technol.* **15,** S8–S16 (2006).
16. Siegman, A. E. *Lasers* (University Science Books, 1986).
17. Ketterle, W., Durfee, D. S. & Stamper-Kurn, D. M. in *Bose–Einstein Condensation in Atomic Gases* (eds Inguscio, M., Stringari, S. & Wieman, C. E.) CXL, 67–176 (Proceedings of the International School of Physics "Enrico Fermi", IOS Press, 1999).
18. De Angelis, E., De Martini, F. & Mataloni, P. Microcavity superradiance. *J. Opt. B* **2,** 149–155 (2000).
19. Yokoyama, H. & Brorson, S. D. Rate equation analysis of microcavity lasers. *J. Appl. Phys.* **66,** 4801–4805 (1989).
20. Bagnato, V. & Kleppner, D. Bose-Einstein condensation in low-dimensional traps. *Phys. Rev. A* **44,** 7439–7441 (1991).
21. Mullin, W. J. Bose-Einstein condensation in a harmonic potential. *J. Low-Temp. Phys.* **106,** 615–641 (1997).
22. Lakowicz, J. R. *Principles of Fluorescence Spectroscopy* 2nd edn, 6 (Kluwer Academic/Plenum, 1999).
23. Hadzibabic, Z. & Dalibard, J. Two-dimensional Bose fluids: an atomic physics perspective. Preprint at ⟨http://arxiv.org/abs/0912.1490⟩ (2009).
24. Hadzibabic, Z., Krüger, P., Cheneau, M., Battelier, B. & Dalibard, J. Berezinskii–Kosterlitz–Thouless crossover in a trapped atomic gas. *Nature* **441,** 1118–1121 (2006).
25. De Martini, F. & Jacobovitz, G. R. Anomalous spontaneous–stimulated-decay phase transition and zero-threshold laser action in a microscopic cavity. *Phys. Rev. Lett.* **60,** 1711–1714 (1988).
26. Yokoyama, H. *et al.* Controlling spontaneous emission and threshold-less laser oscillation with optical microcavities. *Quantum Electron.* **24,** S245–S272 (1992).
27. Yamamoto, Y., Machida, S. & Björk, G. Micro-cavity semiconductor lasers with controlled spontaneous emission. *Opt. Quantum Electron.* **24,** S215–S243 (1992).
28. Kocharovsky, V. V. *et al.* Fluctuations in ideal and interacting bose–einstein condensates: from the laser phase transition analogy to squeezed states and Bogoliubov quasiparticles. *Adv. At. Mol. Opt. Phys.* **53,** 291–411 (2006).
29. McCumber, D. E. Einstein relations connecting broadband emission and absorption spectra. *Phys. Rev.* **136,** A954–A957 (1964).
30. Einstein, A. Zur Quantentheorie der Strahlung. *Physik. Zeitschr.* **18,** 121–128 (1917).

Acknowledgements We thank J. Dalibard and Y. Castin for discussions. Financial support from the Deutsche Forschungsgemeinschaft within the focused research unit FOR557 is acknowledged. M.W. thanks the IFRAF for support of a guest stay at LKB Paris, where part of the discussion on interacting two-dimensional photon gases was developed.

Author Contributions J.K. and M.W. contributed to the experimental idea; J.K. carried out the experiments. J.S. contributed to the experimental set-up. All authors analysed the experimental data and discussed the results.

Author Information Reprints and permissions information is available at www.nature.com/reprints. The authors declare no competing financial interests. Readers are welcome to comment on the online version of this article at www.nature.com/nature. Correspondence and requests for materials should be addressed to M.W. (martin.weitz@uni-bonn.de).